Carbon 204 (2023) 17–25

Contents lists available at ScienceDirect

Carbon

journal homepage: www.elsevier.com/locate/carbon

Perspectives for electromagnetic radiation protection with MXenes

Meikang Han [a,b,*], Yury Gogotsi [b,**]

[a] Institute of Optoelectronics and Shanghai Frontiers Science Research Base of Intelligent Optoelectronics and Perception, Fudan University, Shanghai, 200433, China
[b] A. J. Drexel Nanomaterials Institute and Department of Materials Science and Engineering, Drexel University, Philadelphia, PA, 19104, USA

ARTICLE INFO

Keywords:
MXene
Electronic property
Dielectric property
Electromagnetic interference shielding
Microwave absorption

ABSTRACT

The rapid development of communication and electronic technologies has brought forward new and compelling demands for electromagnetic radiation protection. Two-dimensional transition metal carbides and nitrides known as MXenes entered the field in 2016 and have been quickly reshaping it. Here, we provide a perspective on recent progress and challenges of the MXene family for protection against electromagnetic jamming, including electromagnetic interference (EMI) shielding and microwave absorption. We examine the intrinsic electronic and dielectric properties of MXenes, which are of critical importance for fundamental understanding of electromagnetic response. By tracing the state-of-the-art design strategies, we explore how to optimize MXene-based EMI shielding and microwave absorption materials. Particularly, we highlight the metrics and fundamental mechanisms of electromagnetic protection, aimed to clarifying common misconceptions, and objectively assess the performance of the reported materials. Finally, we discuss challenges to be addressed and give an outlook to future opportunities in the development of MXenes for electromagnetic radiation protection.

1. Introduction

Electromagnetic (EM) radiation is ubiquitous, resulting from electrotechnical, electronic and wireless communication technologies, from cables to integrated circuits, and from cell phones to satellites [1,2]. To reduce the unwanted interference from EM radiation sources, it is essential to either reflect or absorb the incident EM waves. Hence, EM protection materials are generally comprised of two types: electromagnetic interference (EMI) shielding materials that provide both, reflection and absorption of EM waves (e.g., metals), and EM wave absorption materials, which are dominated by absorption (e.g., ferrites) [3]. With the growing demand for light weight and frequency selection, carbon materials (graphene, nanotubes, fibers, carbon black, *etc.*) were extensively explored for EM protection in past two decades [4–8]. Particularly, low-dimensional carbons (e.g., reduced graphene oxide and carbon nanotubes) which have anisotropic charge transport and modifiable surface, facilitated the design of architectures for microwave attenuation [9]. Nevertheless, compared with carbon-based microwave absorption materials, thin EMI shields made with carbons are less effective, presumably due to their limited electrical conductivity.

MXenes, a large class of two-dimensional (2D) transition metal carbides or nitrides, were reported in 2011 and quickly developed into a very large family of materials with dozens of compositions reported to date [10,11]. In 2016, $Ti_3C_2T_x$ MXene was reported to exhibit EMI shielding effectiveness (SE) of 92 dB at a thickness of 45 μm, making it a highly promising shielding material [12]. Almost at the same time, $Ti_3C_2T_x$ was also demonstrated to be efficient microwave absorber at gigahertz frequencies after moderate surface modification [13]. Since then, MXenes have become a game changer in the field of EM protection materials. Generally, MXenes are obtained by the removal of A-layer atoms from their parent MAX phases. Hence, MXenes inherit the metallic conductivity of the carbide and nitride precursors [14,15]. Moreover, the top-down synthesis with acid etching endows MXenes with abundant surface functionalities (-O, -F, -OH, *etc.*), which make MXenes hydrophilic and processable from aqueous solutions. Meanwhile, the polar and negatively charged MXene surfaces facilitate the intercalation of various cations or organic molecules, such as Li^+, NH_4^+, or dimethylsulfoxide [16–19]. This offers the possibility to modify the surfaces and form complex heterostructures. In contrast to the simple chemistry of graphene, these features, coupled with the variety of compositions and number/structure of atomic layers, allow tunability of electronic and dielectric properties of MXenes, which play crucial roles

* Corresponding author. Institute of Optoelectronics and Shanghai Frontiers Science Research Base of Intelligent Optoelectronics and Perception, Fudan University, Shanghai, 200433, China.
** Corresponding author.
E-mail addresses: mkhan@fudan.edu.cn (M. Han), gogotsi@drexel.edu (Y. Gogotsi).

https://doi.org/10.1016/j.carbon.2022.12.036
Received 14 November 2022; Received in revised form 11 December 2022; Accepted 11 December 2022
Available online 13 December 2022

in EM protection performance.

The general formula of MXenes is $M_{n+1}X_nT_x$, where M represents early transition metals, X is C and/or N, T_x is the surface termination (-O, -OH, halogens, chalcogens, or their mix), and n = 1–4 [20–22]. The wide variety and tunability of MXene compositions and structures, including the change of M and/or X element, the control of the surface chemistry (T_x), and the modification of the number of atomic layers (*n*), determine the diverse MXene family in which more than 40 stoichiometric MXene compositions and numerous solid solutions have already been synthesized, and an almost infinite number of compositions should be possible [23–25]. However, over the past five years, more than 90% of all MXene-related EM protection research focused on $Ti_3C_2T_x$ MXene. In addition, while research efforts are currently directed towards $Ti_3C_2T_x$-based hybrids/composites for the optimization of EM protection capability, such as $Ti_3C_2T_x$/polymers, $Ti_3C_2T_x$/magnetic particles, and $Ti_3C_2T_x$/carbons [26–30], the fundamental understanding of electronic and dielectric properties of pristine MXenes is still lacking.

While the intrinsic properties of diverse MXenes for EM protection are essential, there is an urgent need to clarify some concepts and metrics for the evaluation of EMI shielding and microwave absorption materials [31,32]. EM radiation protection is becoming one of the most promising applications for MXenes. More than 500 research publications about MXenes for EMI shielding or microwave absorption appeared in the past three years (Source: Web of Science). As the community grows rapidly, it is important to properly report and interpret the experimental results. Achieving the fundamental understanding of interactions between MXenes and EM waves would have far-reaching benefits.

In the following sections, we discuss the essential electronic and dielectric characteristics of MXenes and summarize the key advances in MXene-based EM protection materials over the past six years. While several reviews have covered MXene-based shields and MXene-based microwave absorbers [26,27,33], we center our discussion around the role of MXenes in the EM responses to dig into the effective routes for EM protection enhancement. Specifically, combining the merits of MXenes in EM protection, we examine the scientifically justified metrics for comparison and optimization of the effectiveness in reflection and absorption. Finally, we provide an outlook to challenges and new opportunities of EM protection with MXenes for future research.

2. Electronic and dielectric properties of MXenes

2.1. Electronic properties

As EMI shielding performance is directly related to the electrical conductivity of materials, it is essential to optimize the electronic transport in MXene-based shields [34,35]. Electronic properties of MXenes have been extensively explored computationally [23,36–38]. However, electronic transport in MXenes varies with compositions, surface terminations, defects, layer arrangement, *etc.*, which are not easy to model. Here we only examine the experimental results for MXene flakes, MXene films, and MXene-based composites.

Before discussing the conductivity of MXene films, it is critical to understand the intrinsic transport in single 2D flakes, which was measured with a field-effect transistor (FET) device (Fig. 1a). The electrical conductivity of monolayer $Ti_3C_2T_x$ flake reached 11,000 S cm^{-1} and the field-effect electron mobility was up to 6 cm^2 V^{-1} s^{-1} (Fig. 1b) [39]. It showed an improvement by a factor of two compared with the first study of similar $Ti_3C_2T_x$ FETs, which is attributed to the improved stoichiometry of MXene [40]. However, it is lower than the conductivity of $Ti_3C_2T_x$ films (>20,000 S cm^{-1}) which was made of stacked $Ti_3C_2T_x$ flakes by vacuum-assisted filtration [41]. For the monolayer $Ti_3C_2T_x$ with a larger flake size (>10 μm), the electrical conductivity and the electron mobility were 6,500 S cm^{-1} and 4.2 cm^2 V^{-1} s^{-1}, respectively [42]. The reported electrical conductivity of $Nb_4C_3T_x$ monolayer was about 1,024 S cm^{-1}, which is higher than that of $Nb_4C_3T_x$ films [43,44]. The fabrication of FET devices and variations in the quality of MXenes

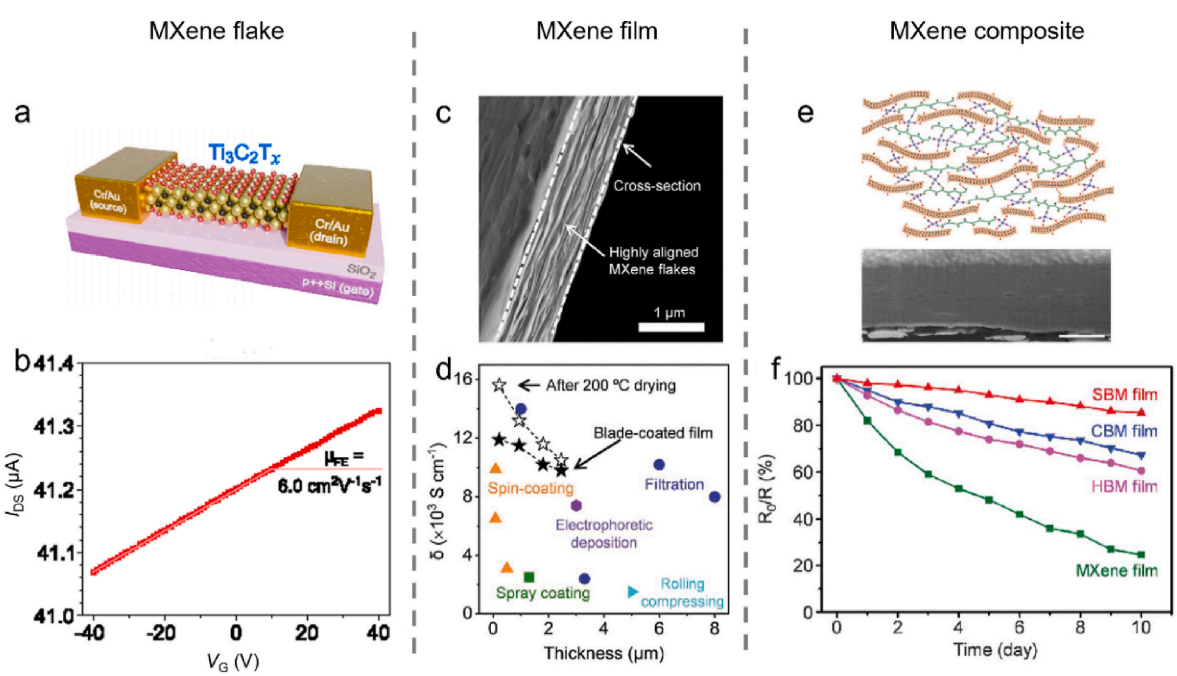

Fig. 1. Electronic properties of MXenes. *MXene flake*: (a) Schematic of a two-terminal device with a $Ti_3C_2T_x$ channel, showing the electronic measurement on a single MXene flake; (b) Two-terminal transfer characteristics of a monolayer $Ti_3C_2T_x$ field-effect transistor. V_{DS} = 0.1 V. Reprinted with permission from Ref. [39], Copyright Elsevier 2021. *MXene film*: (c) SEM image of the cross-section of a blade-coated $Ti_3C_2T_x$ film with highly aligned MXene flakes; (d) Comparison of the electrical conductivity as a function of film thicknesses for $Ti_3C_2T_x$ films prepared using different methods, including spin coating, spray coating, filtration, electrophoretic deposition, and rolling compressing. Reprinted with permission from Ref. [66], Copyright Wiley-VCH 2020. *MXene composite*: (e) Structure schematic and SEM image of the cross-section of sequentially bridged MXene (SBM) film with sodium carboxymethyl cellulose; (f) Conductance retention percentage as a function of time for different MXene films, including pure MXene, covalently bridged MXene (CBM), hydrogen-bonded MXene (HBM), and SBM films in humid air. Reprinted with permission from Ref. [62], Copyright AAAS 2021. (A colour version of this figure can be viewed online.)

(defects, oxidation, *etc.*) may affect the measured properties of individual MXene flakes. Thus, additional measurements on pristine MXene flakes of various MXene compositions and with various surface chemistries are needed.

Electron transport in MXene films is more complicated as there is a convolution of intraflake and interflake effects. First, with the improvement of MXene quality (stoichiometry, minimization of defects, increase in flake size, *etc.*) in recent years, the conductivity of $Ti_3C_2T_x$ film showed a significant increase to over 20,000 S cm^{-1} [41,45]. Second, MXene films have been manufactured using various techniques, including spin coating [46], spray coating [47], drop casting [48], inkjet printing [49], screen printing [50], interfacial assembly, *etc.* [51–55], owing to easy solution processibility of MXenes. Different processes lead to differences in arrangements/alignment of MXene flakes in the film, which have a profound effect on the conductivity. For example, blade-coating method can produce $Ti_3C_2T_x$ films with highly aligned flakes, when a liquid crystalline MXene dispersion is used (Fig. 1c). Compared with vacuum-filtered films (~9,860 S cm^{-1}), the conductivity of blade-coated $Ti_3C_2T_x$ film showed a significant increase (~15,100 S cm^{-1}) (Fig. 1d). The interflake intercalants in MXene films also affect the electron transport. Li^+-intercalated V_2CT_x film after ion exchange was more conductive than the tetramethylammonium ion-intercalated film [56]. The removal of intercalant ions and partial removal of surface groups after vacuum annealing also decreased the film resistance [57]. In addition, although MXenes are metallic, the interflake electron hopping process makes the temperature-dependent behavior of the film conductivity unique. The resistance decreases with the increasing temperature at 10–300 K, resembling the trend for semiconductors rather than metals [23,58,59]. Hence, the conductivity of MXene films can be adjusted by the modulation of intercalation, surface termination, and flakes arrangement.

MXene composite films with various polymers have higher mechanical strength and environmental stability compared to neat MXenes [60]. However, the introduction of polymer between MXene flakes affects the conductive network. Two strategies are effective to optimize the conductivity through enhancing the carriers transport channels. Wan et al. densified MXene films through sequential bridging of hydrogen and covalent bonding agents, leading to strong and highly conductive MXene composites (Fig. 1e) [61,62]. The conductivity of sequentially bridged MXene (SBM) films with sodium carboxymethyl cellulose reached >6,000 S cm^{-1} and was retained in humid environment (Fig. 1f), which was attributed to compact and aligned layers with few voids. Another approach is making laminated structures using layer-by-layer assembly [63,64]. For instance, laminated cellulose nanofiber/$Ti_3C_2T_x$ films maintain the high mechanical strength (>250 MPa) and low resistance (3.1 Ω □$^{-1}$), leading to an EMI SE value of 60 dB at a thickness of 7.7 μm [64]. Semi-transparent $Ti_3C_2T_x$/carbon nanotube films fabricated by spin spray layer-by-layer deposition showed a conductivity of 130 S cm^{-1} at nanometer-scale thickness [65]. High alignment of MXene layers in composite films facilitates the formation of local conductive network and the electron hopping. The conductivity of MXene films has been improved with the optimized synthesis of MXenes and rational structural designs. Still, the fundamental understanding of intraflake and interflake electron transport is incomplete. Besides MXene/polymer composites, incorporating MXene into ceramic matrix could be effective approach for high-temperature EMI shielding [35].

2.2. Dielectric properties

Dielectric properties are important for designing microwave absorption materials, especially for non-magnetic microwave absorbers. Since MXene-based microwave absorbers attracted tremendous attention, there are numerous reports on the permittivity of MXene-based absorbers at gigahertz frequencies (mostly 2–18 GHz). However, few investigations of dielectric properties outside this frequency range have been reported. In this regard, we briefly summarize the dielectric properties of MXenes in a broad range of frequencies, which may inspire the community to explore the frequency-dependent EM responses of MXenes in depth.

In visible and near infrared (Vis-NIR) ranges, the dielectric constant of MXene films is usually measured with spectroscopic ellipsometry. The real part turns to be negative with the increasing wavelength, indicating the onset of free carrier oscillations in $Ti_3C_2T_x$ films (Fig. 2a). A similar trend was observed for Ti_2CT_x, V_2CT_x, and $V_4C_3T_x$ films, suggesting their metallic nature [36,67]. When the frequency is extremely low (e.g., kHz), the permittivity significantly increases with the increasing filler loading of $Ti_3C_2T_x$ in polymer matrix, but the dielectric loss is low when the filler loading is < 10 wt% (Fig. 2b) [68]. The dielectric enhancement is attributed to the accumulation of charges at the interfaces which forms the dipoles [69]. Similarly, at gigahertz ranges, when a tiny amount of $Ti_3C_2T_x$ (~2 wt%) is introduced in a polymer, the real permittivity is high (up to 73), but the dielectric loss is only 0.09 (Fig. 2c and 2d) [70]. This feature of $Ti_3C_2T_x$/polymer composites has been repeatedly demonstrated in the literature [13,71]. It indicates that pristine $Ti_3C_2T_x$ is not a promising candidate for microwave absorption, which will be discussed in detail in the next section.

It is worth noting that there is still a lack of systematic investigation of dielectric properties of various MXenes in different frequency ranges. As the operation frequencies of electronic devices vary, it is important to consider the EM protection in a broad or a specific frequency range. There is much room for adjusting the dielectric response of MXenes on demand, which is critical for the electromagnetic wave absorption rather than only 'microwave' absorption.

3. MXene for electromagnetic protection

While the EM protection with MXenes attracts extensive attention, some readers, especially newcomers to the field, may get confused with the concepts of EMI shielding and microwave absorption. The most common misinterpretation is that microwave absorption can be treated as EMI shielding and the same metrics are used to index the performance. In principle, both refer to the basic responses to the incident EM waves (reflection, absorption, and transmission). However, they are calculated based on different models and equations. We clarify these concepts in combination with the discussion of MXene-based EMI shielding and microwave absorption materials in the following sections.

3.1. MXene for EMI shielding

Compared with conventional metal shields, the merit of MXenes is the feasibility of manufacturing flexible (bendable and foldable) thin films for effective EMI shielding. Films starting from 1 μm in thickness can be used freestanding. By interfacial self-assembly, Yun et al. reported EMI shielding behavior of $Ti_3C_2T_x$ films, monolayer-by-monolayer (Fig. 3a–c) [72]. It shows that a monolayer $Ti_3C_2T_x$ film shields ~20% of electromagnetic waves and a 24-layer film (~55 nm thick) can achieve effective shielding (EMI SE > 20 dB). With the improved quality of MXene, sprayed $Ti_3C_2T_x$ film reached EMI SE of 21 dB at a thickness of only ~40 nm, owing to the high conductivity (~14, 000 S cm^{-1}) and good interflake contacts [73]. Although $Ti_3C_2T_x$ films have the best shielding performance so far, many other MXene compositions with high conductivity are promising as well, including Ti_2CT_x, Ti_3CNT_x, V_2CT_x, $Mo_2TiC_2T_x$, $Mo_2Ti_2C_3T_x$, $Nb_4C_3T_x$, and $V_4C_3T_x$ (Fig. 3d and 3e) [36,73,74]. Particularly, Ti_3CNT_x films after thermal annealing have a higher absorption effectiveness than $Ti_3C_2T_x$ films, although their conductivity is lower [74]. This may be attributed to its metamaterial-like architecture with voids between the layers. With the emergence of new MXene compositions and the optimization of synthesis, it is believed that more members in the MXene family can be used for EMI shielding and further developed into multifunctional films with superior and selective shielding properties, depending on specific

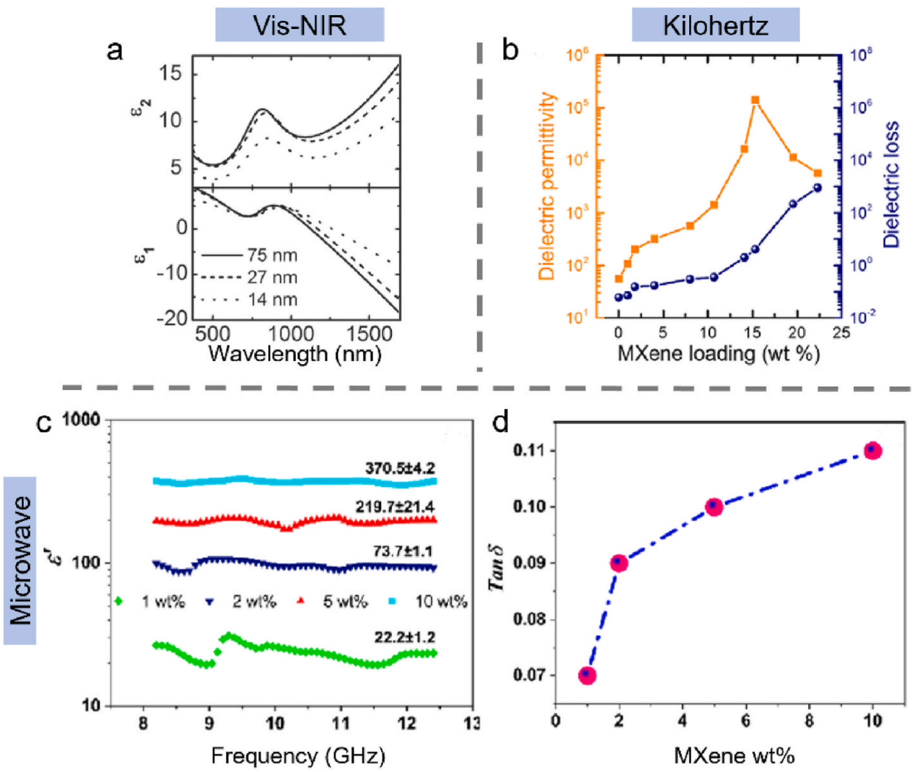

Fig. 2. Dielectric properties of MXenes. (a) Imaginary (top) and real (bottom) permittivity of $Ti_3C_2T_x$ films in the vis-NIR range. Reprinted with permission from Ref. [46], Copyright Wiley-VCH 2016. (b) The permittivity and dielectric loss of the MXene/polymer composites with different ratios of MXene loading at 1 kHz. Reprinted with permission from Ref. [68], Copyright American Chemical Society 2018. (c) The real permittivity (ε') and (d) dielectric loss (tan δ) of the MXene/polyvinyl alcohol composites with different MXene loadings at 8.2–12.4 GHz. Reprinted with permission from Ref. [70], Copyright American Chemical Society 2019. (A colour version of this figure can be viewed online.)

characteristics of individual MXenes.

Owing to the active surface and high Young's modulus (~0.33 TPa) [75], MXene composite films, such as MXene/Ag nanowire films [76–78], MXene/carbon nanotube films [65,79,80], and MXene/cellulose films [62,81–84], with optimized EMI shielding capability and mechanical strength were developed. Chen et al. fabricated transparent MXene/Ag nanowire films with enhanced interconnection by welding the nanowire junctions (Fig. 3f and 3g) [77]. The flexible film with a visible transmittance of ~83% achieved an EMI SE value of 49 dB, allowing applications in integrated electronics and smart windows. For personal EM protection, MXene-coated fabrics with simple dip-coating process are a promising alternative to currently used metal wires [85]. Considering their scalability, mechanical properties, and adhesion, MXene composite films offer promise for practical applications.

Porous design is an effective approach to modulating the reflection and absorption of incident EM waves. Various MXene-based foams have been developed to obtain lightweight, compressible/stretchable EMI shields with weak reflection. Pure MXene aerogels with aligned lamellar architecture maintain a stress recovery of >80% and stable electrical resistance after compression cycles. Meanwhile, the ratio of reflection to absorption is tunable with compression and the total shielding effectiveness is maintained [86]. Hydrazine-induced MXene foams have SE_A (SE of absorption) below 5 dB, while the total EMI SE reaches 70 dB. It demonstrates a significant contribution of porous structure to the EM wave absorption. With additives, MXene foam shields can be further optimized. For example, compressible MXene/polyaniline foam presents an EMI SE of ~24–40 dB, but its reflection coefficient is only ~0.2–0.3 [87]. MXene/reduced graphene oxide aerogel with a small $Ti_3C_2T_x$ amount of 0.74 vol% achieved an EMI SE of >50 dB, owing to its regular cellular structure [88]. Furthermore, the MXene/graphene oxide aerogel was also effective for shielding in the terahertz range [89].

Following the discussion on the ratio of reflection to absorption, the "absorption-dominated mechanism" is frequently mentioned in the literature. However, in many cases, this claim is misleading, especially for MXene-based shields, because the physical meaning behind calculations is neglected [31]. This is not a new issue but it should be addressed. EMI SE, which is the core parameter to evaluate EMI shielding capability, is represented on a logarithmic scale, as shown in the following equations:

$$SE_{total} = 10\log_{10}\left(\frac{1}{T}\right) \tag{1}$$

$$SE_{R} = 10\log_{10}\left(\frac{1}{1-R}\right) \tag{2}$$

$$SE_{A} = 10\log_{10}\left(\frac{1-R}{T}\right) \tag{3}$$

where A, R, and T are absorption, reflection, and transmission power, respectively ($A + R + T = 1$). SE_{total}, SE_R, and SE_A represent the total, reflection, and absorption effectiveness, respectively.

Most EMI shielding materials have high electrical conductivity, which leads to strong reflection (high R). Moreover, when SE_R is only 10 dB, R value is 0.9 apparently. It means that >90% of incident EM waves are reflected. In other words, although SE_A can be significantly increased, the real absorption (A) contribution just has a slight change in most cases. As a result of this deceptive calculation, the real ratios of reflection and absorption are often neglected. We advocate for a scientific and rigorous description on the contribution of reflection and absorption to EMI shielding. In principle, only when SE_R is < 3 dB ($R < 50\%$), the shielding mechanism can be considered as absorption-dominated [32]. When the effect of absorption is emphasized specifically, it is necessary to provide A and R values, which explicitly show the ratio between absorption and reflection. Moreover, in term of shielding mechanisms, the EM absorption contribution should not be overrated when the absorption ratio is low.

3.2. MXene for microwave absorption

While the excellent shielding capability of MXene films is mainly achieved by the EM wave reflection, efficient EM wave absorption

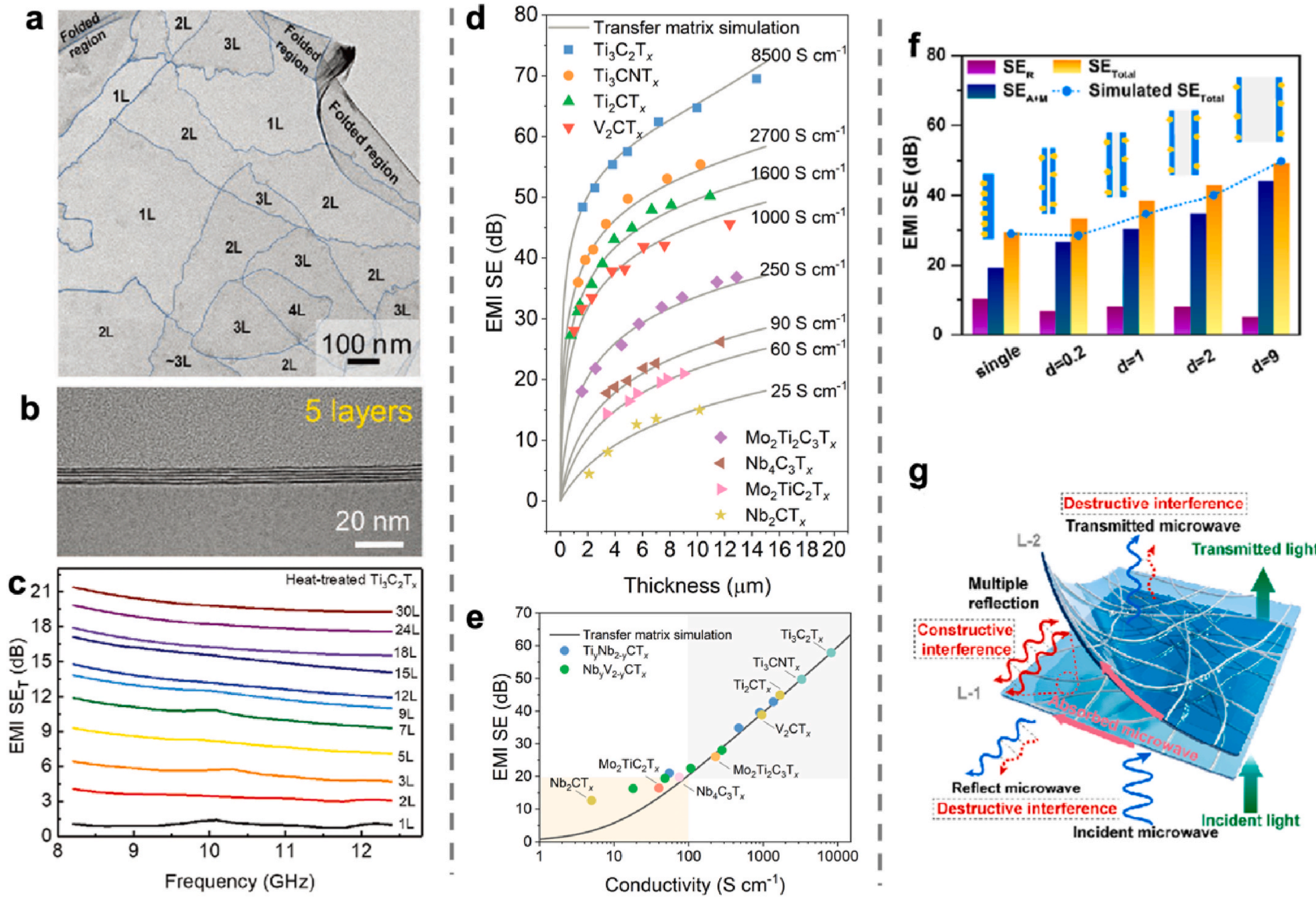

Fig. 3. EMI shielding with MXene films. (a) TEM image of a monolayer assembled $Ti_3C_2T_x$ film. (b) Cross-sectional TEM image of a five-layer assembled $Ti_3C_2T_x$ film, showing the flakes alignment. (c) EMI SE of $Ti_3C_2T_x$ films varied with the number of layers. Reprinted with permission from Ref. [72], Copyright Wiley-VCH 2020. (d) Thickness-dependent EMI SE of various MXene films. (e) The relationship between EMI SE and the electrical conductivity of MXenes. Reprinted with permission from Ref. [73], Copyright American Chemical Society 2020. (f) EMI SE of $Ti_3C_2T_x$/Ag nanowire (MA) films and double MA films with various gap distances. (g) Schematic of the EMI shielding behavior of a double transparent MA film, such as $Ti_3C_2T_x$/Ag nanowire film, for EMI shielding. Reprinted with permission from Ref. [77], Copyright American Chemical Society 2020. (A colour version of this figure can be viewed online.)

without secondary EM pollution is desired. Due to the metallic conductivity of MXenes, MXene-based microwave absorption materials are generally the composites that mix MXene with microwave-transparent polymers to weaken impedance mismatching with free space. Before tackling the question of microwave absorption enhancement with MXenes, it is worth mentioning the basic calculations for microwave absorption. Generally, reflection loss (or return coefficient) value is used to evaluate the microwave attenuation, which is different from the "EMI SE" for EMI shielding. It is based on the metal back panel model and transmission-line theory [90]. Reflection loss (*RL*) is directly determined by the permittivity and permeability of materials rather than the conductivity. The calculation equations are as follows:

$$RL\ (\text{dB}) = 20\ log_{10}|(Z_{\text{in}} - 1) / (Z_{\text{in}} + 1)| \quad (4)$$

$$Z_{\text{in}} = \sqrt{\frac{\mu}{\varepsilon}} tanh\left(j2\pi\sqrt{\mu\varepsilon}fd / c\right) \quad (5)$$

where Z_{in} is the normalized input impendence of the microwave absorption layer, ε and μ are the permittivity and permeability, f is the EM wave frequency, d is the absorption layer thickness, c is the light velocity in vacuum. $RL < -10$ dB means that >90% of microwaves energy is absorbed (dissipated as heat).

In light of the dielectric properties of MXenes that we discussed above, pristine $Ti_3C_2T_x$ composites have poor microwave attenuation ability. Hence, in recent years, the main strategy was to introduce additional absorbers along with the architecture design (material architectonics) to improve the dielectric loss of $Ti_3C_2T_x$. Magnetic materials, such as magnetic metal particles (Fe, Co, Ni, and alloys) and magnetic oxides (Fe_2O_3, Fe_3O_4, and ferrites) [30,80,91–94], carbon materials (carbon nanotube/fiber, reduced graphene oxide, graphite, *etc.*) [95–99], high-loss semiconductors (SiC, MoS_2, *etc.*) or multiple additives were used [100–103].

Wen et al. assembled double-shell MXene@Ni microspheres with outer Ni nanospikes and inner MXene flakes, enabling the additional magnetic loss (Fig. 4a and 4b) [94]. The effective absorption bandwidth reached 4.48 GHz (13.52–18 GHz) at a thickness of 1.5 mm (Fig. 4c). The formation of electro-magnetic heterogeneous interfaces facilitates the charge accumulation, which contributes to the microwave dissipation under an alternating EM field. While additional magnetic phases induce magnetic loss, adding carbons or semiconductors can optimize the permittivity and enhance dielectric loss. Li et al. reported lightweight $Ti_3C_2T_x/MoS_2$ self-rolling rods with improved polarization loss, which achieved the effective absorption over the whole X-band (8.2–12.4 GHz) (Fig. 4d–f) [103]. MoS_2 rods hinder the construction of conductive network but balance the dielectric loss, enhancing the relaxation along with hierarchical interfaces. In addition, foam structure is another approach to improving the microwave absorption with better impedance match and inner scattering [104,105]. These strategies

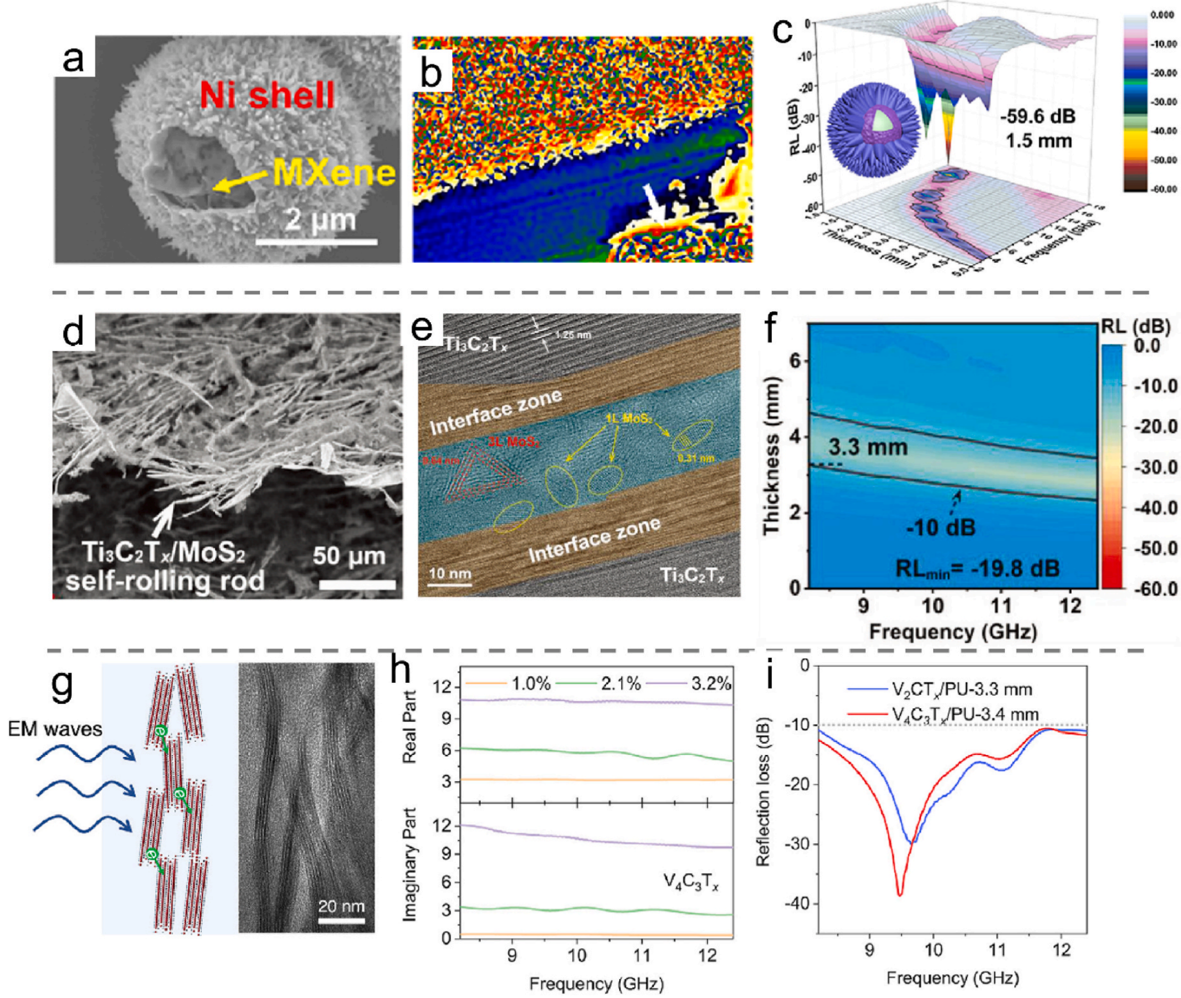

Fig. 4. MXenes for microwave absorption. *MXene/magnetic material*: (a) SEM image of a $Ti_3C_2T_x$/Ni microsphere. (b) off-axis electron hologram of $Ti_3C_2T_x$/Ni interface, showing the charge density distribution. (c) Microwave absorption performance of $Ti_3C_2T_x$/Ni microspheres. Reprinted with permission from Ref. [94], Copyright American Chemical Society 2021. *MXene/non-magnetic material*: (d) SEM image of $Ti_3C_2T_x/MoS_2$ foam showing the self-rolling rod structure. (e) TEM image of $Ti_3C_2T_x/MoS_2$, showing the interface between $Ti_3C_2T_x$ and MoS_2. (f) Microwave absorption performance of $Ti_3C_2T_x/MoS_2$ foam. Reprinted with permission from Ref. [103], Copyright Wiley-VCH 2022. *$V_{n+1}C_nT_x$ MXene*: (g) Schematic and TEM image of $V_4C_3T_x$ MXene in polyurethane, showing the aligned MXene flakes. (h) Permittivity of $V_4C_3T_x$/polyurethane composites. (i) Microwave absorption performance of $V_{n+1}C_nT_x$/polyurethane composite, showing the effective absorption in the whole X-band. Reprinted with permission from Ref. [36], Copyright Elsevier 2022. (A colour version of this figure can be viewed online.)

indicate that the principle of designing MXene-based microwave absorbers is to obtain a synergetic effect of dielectric loss, magnetic loss, and conductive loss with moderate conductivity, which is different from EMI shields with high conductivity. Owing to the 2D layers, native defects, and abundant functional groups of MXene, dielectric properties of MXene-based absorbers dominate the internal EM response, including transport of electrons and formation of dipoles at multiple hetero-interfaces [106–108]. The polarization relaxation of dipoles at the interfaces and defects contributes greatly to the consumption of incident EM waves energy. Therefore, defect engineering and surface modification could be effective routes to adjust dielectric properties and enhance microwave absorption.

While tremendous effort was made to modulate microwave attenuation of $Ti_3C_2T_x$, there are only a handful of studies that have attempted to explore other MXenes as microwave absorbers [36,109]. Recently, it was found that V-based MXenes (V_2CT_x and $V_4C_3T_x$) have efficient dielectric loss and lower conductivity (~1,000 S cm^{-1} for films) than $Ti_3C_2T_x$, providing an advantageous balance between microwave absorption and impedance match (Fig. 4g and 4h) [36]. $V_{n+1}C_nT_x$/polyurethane composites with an ultralow loading (~2 wt%) exhibited efficient EM wave absorption in the whole X band (Fig. 4i). Both $Ti_3C_2T_x$ and $V_{n+1}C_nT_x$ have abundant surface groups, free electron transport, native defects, and 2D nature, which have profound effects on the optimization of microwave attenuation. However, the proper dielectric and electronic properties make $V_{n+1}C_nT_x$ MXenes more promising as microwave absorbers.

As numerous MXene-based and carbon-based microwave absorbers have emerged in recent years, it is important to report proper metrics for evaluating microwave absorption performance. Generally, the minimum reflection loss (RL_{min}), the effective bandwidth, the absorber thickness, and the filler loading ratio are the main metrics used in the literature. However, sometimes these parameters are deceptive and cannot accurately reflect the scientific merit behind the work. First, the RL_{min} value is not suggested to be overrated in the reports, when it meets the standard of effective absorption. Because, in most practical scenarios, there may be no significant difference between −30 dB (99.9% absorption) and −70 dB (99.99999% absorption). Second, the broad effective bandwidth is significant. However, it is noteworthy that it is easier to achieve broader bandwidth at higher frequency range (e.g., 12–18 GHz). Therefore, it is meaningful to specify the frequency range of effective bandwidth and put efforts to enhance absorption at lower frequencies, which are important in many applications. Third, the filler loading ratio of absorber is often neglected, although it is critical for the practical applications, when pursuing minimal cost and simple manufacturing.

4. Conclusions and outlook

We offer our perspective on the key challenges and potential opportunities for the development of MXene-based EM protection. While only about 6 years passed since the first report on EMI shielding with MXenes, MXenes have already demonstrated significant promise for EM radiation protection. Improved fundamental understanding of the EM responses of MXenes and their interaction with EM waves will be needed for predictive modeling and computational design of MXene-based shields utilizing a variety of already known and potentially available MXenes.

Although improvements in specific performance have been achieved, we still know little about the electronic and dielectric properties of pristine MXenes in different frequency ranges. Future studies should concentrate on building physical models and systematic measurements, as 2D MXenes have shown differences from the bulk materials under an alternating EM field. It is helpful to understand the interactions of MXenes with EM waves, extending the application scenarios beyond gigahertz range, especially towards lower frequencies.

While numerous studies focused on $Ti_3C_2T_x$, it is reasonable to investigate the large MXene family beyond $Ti_3C_2T_x$, especially since $Ti_3C_2T_x$ is not ideal for microwave absorption. The potential of other MXenes has been well demonstrated, e.g., Ti_3CNT_x for EMI shielding and $V_{n+1}C_nT_x$ MXenes for microwave absorption. Solid solution MXenes could be candidates for modulation of electronic and dielectric properties by the substitution of M-site or X-site elements. More broadly, high-entropy MXenes may offer further ways to control the EM responses, although the study just started. With the continuous expansion of the MXene family, it is essential to conduct systematic investigations on the basic physical properties that will allow selection of building blocks for developing MXene-based EM protection. Moreover, utilizing specific properties of different MXenes may enable development of multifunctional MXene shields.

Finally, the chemical and thermal stability of MXenes have been improved in the past decade. However, the reliability and scale-up of high-quality MXenes will require further efforts to meet industry expectations. While there is a strong desire to commercialize MXenes in protection of integrated electronics, more sophisticated approach to manufacturing MXene films/coatings and their encapsulation should be explored to ensure stable operation under variable environmental conditions, that may include high humidity, elevated temperatures, sunlight, *etc*. Meanwhile, it is important to further improve mechanical properties of MXene films/coatings, such as adhesion, tensile strength, *etc*.

Last but not least, given the 2D nature of MXenes, their unique electronic transport properties, large and highly polar surface, we envision that the use of MXene for metasurface design could potentially open new avenues for selective reflection and absorption with ultrathin and flexible films in a broad frequency range, which is impossible with traditional EM radiation protection materials. The active control of EM response with MXenes could make a huge impact on many fields.

Declaration of competing interest

The authors declare that they have no known competing financial interests or personal relationships that could have appeared to influence the work reported in this paper.

Data availability

Data will be made available on request.

Acknowledgements

This work was supported by the U.S. National Science Foundation (grant ECCS-2034114). M.H. acknowledges the support from Shanghai Pujiang Program (22PJ1400800).

References

[1] S. Dang, O. Amin, B. Shihada, M.-S. Alouini, What should 6G be? Nat. Electron. 3 (2020) 20–29.
[2] M. Médard, Is 5 just what comes after 4? Nat. Electron. 3 (2020) 2–4.
[3] X. Yin, L. Kong, L. Zhang, L. Cheng, N. Travitzky, P. Greil, Electromagnetic properties of Si–C–N based ceramics and composites, Int. Mater. Rev. 59 (2014) 326–355.
[4] H. Sun, R. Che, X. You, Y. Jiang, Z. Yang, J. Deng, L. Qiu, H. Peng, Cross-stacking aligned carbon-nanotube films to tune microwave absorption frequencies and increase absorption intensities, Adv. Mater. 26 (2014) 8120–8125.
[5] R.C. Che, L.-M. Peng, X.F. Duan, Q. Chen, X.L. Liang, Microwave absorption enhancement and complex permittivity and permeability of Fe encapsulated within carbon nanotubes, Adv. Mater. 16 (2004) 401–405.
[6] Z. Chen, C. Xu, C. Ma, W. Ren, H.M. Cheng, Lightweight and flexible graphene foam composites for high-performance electromagnetic interference shielding, Adv. Mater. 25 (2013) 1296–1300.
[7] B. Wen, M. Cao, M. Lu, W. Cao, H. Shi, J. Liu, X. Wang, H. Jin, X. Fang, W. Wang, Reduced graphene oxides: light-weight and high-efficiency electromagnetic interference shielding at elevated temperatures, Adv. Mater. 26 (2014) 3484–3489.
[8] M. Han, X. Yin, W. Duan, S. Ren, L. Zhang, L. Cheng, Hierarchical graphene/SiC nanowire networks in polymer-derived ceramics with enhanced electromagnetic wave absorbing capability, J. Eur. Ceram. Soc. 36 (2016) 2695–2703.
[9] M.S. Cao, X.X. Wang, M. Zhang, J.C. Shu, W.Q. Cao, H.J. Yang, X.Y. Fang, J. Yuan, Electromagnetic response and energy conversion for functions and devices in low-dimensional materials, Adv. Funct. Mater. 29 (2019), 1807398.
[10] M. Naguib, M. Kurtoglu, V. Presser, J. Lu, J. Niu, M. Heon, L. Hultman, Y. Gogotsi, M.W. Barsoum, Two-dimensional nanocrystals produced by exfoliation of Ti_3AlC_2, Adv. Mater. 23 (2011) 4248–4253.
[11] A. VahidMohammadi, J. Rosen, Y. Gogotsi, The world of two-dimensional carbides and nitrides (MXenes), Science 372 (2021), eabf1581.
[12] F. Shahzad, M. Alhabeb, C.B. Hatter, B. Anasori, S.M. Hong, C.M. Koo, Y. Gogotsi, Electromagnetic interference shielding with 2D transition metal carbides (MXenes), Science 353 (2016) 1137–1140.
[13] M. Han, X. Yin, H. Wu, Z. Hou, C. Song, X. Li, L. Zhang, L. Cheng, Ti_3C_2 MXenes with modified surface for high-performance electromagnetic absorption and shielding in the X-band, ACS Appl. Mater. Interfaces 8 (2016) 21011–21019.
[14] M. Sokol, V. Natu, S. Kota, M.W. Barsoum, On the chemical diversity of the MAX phases, Trends in Chemistry 1 (2019) 210–223.
[15] K.R.G. Lim, M. Shekhirev, B.C. Wyatt, B. Anasori, Y. Gogotsi, Z.W. Seh, Fundamentals of MXene synthesis, Nat. Synth. 1 (2022) 601–614.
[16] M. Ghidiu, M.R. Lukatskaya, M.-Q. Zhao, Y. Gogotsi, M.W. Barsoum, Conductive two-dimensional titanium carbide 'clay' with high volumetric capacitance, Nature 516 (2014) 78.
[17] V. Natu, R. Pai, M. Sokol, M. Carey, V. Kalra, M.W. Barsoum, 2D $Ti_3C_2T_z$ MXene synthesized by water-free etching of Ti_3AlC_2 in polar organic solvents, Chem 6 (2020) 616–630.
[18] O. Mashtalir, M. Naguib, V.N. Mochalin, Y. Dall'Agnese, M. Heon, M.W. Barsoum, Y. Gogotsi, Intercalation and delamination of layered carbides and carbonitrides, Nat. Commun. 4 (2013) 1716.
[19] O. Mashtalir, M.R. Lukatskaya, A.I. Kolesnikov, E. Raymundo-Pinero, M. Naguib, M. Barsoum, Y. Gogotsi, The effect of hydrazine intercalation on the structure and capacitance of 2D titanium carbide (MXene), Nanoscale 8 (2016) 9128–9133.
[20] G. Deysher, C.E. Shuck, K. Hantanasirisakul, N.C. Frey, A.C. Foucher, K. Maleski, A. Sarycheva, V.B. Shenoy, E.A. Stach, B. Anasori, Y. Gogotsi, Synthesis of Mo_4VAlC_4 MAX phase and two-dimensional Mo_4VC_4 MXene with five atomic layers of transition metals, ACS Nano 14 (2020) 204–217.
[21] Y. Gogotsi, B. Anasori, The rise of MXenes, ACS Nano 13 (2019) 8491–8494.
[22] Y. Gogotsi, Q. Huang, MXenes: two-dimensional building blocks for future materials and devices, ACS Nano 15 (2021) 5775–5780.
[23] M. Han, K. Maleski, C.E. Shuck, Y. Yang, J.T. Glazar, A.C. Foucher, K. Hantanasirisakul, A. Sarycheva, N.C. Frey, S.J. May, V.B. Shenoy, E.A. Stach, Y. Gogotsi, Tailoring electronic and optical properties of MXenes through forming solid solutions, J. Am. Chem. Soc. 142 (2020) 19110–19118.
[24] M.W. Barsoum, Y. Gogotsi, Removing roadblocks and opening new opportunities for MXenes, Ceram. Int. (2022), https://doi.org/10.1016/j.ceramint.2022.10.051.
[25] V. Kamysbayev, A.S. Filatov, H. Hu, X. Rui, F. Lagunas, D. Wang, R.F. Klie, D. V. Talapin, Covalent surface modifications and superconductivity of two-dimensional metal carbide MXenes, Science 369 (2020) 979–983.
[26] Q. Song, F. Ye, L. Kong, Q. Shen, L. Han, L. Feng, G. Yu, Y. Pan, H. Li, Graphene and MXene nanomaterials: toward high-performance electromagnetic wave absorption in gigahertz band range, Adv. Funct. Mater. 30 (2020), 2000475.
[27] M.-S. Cao, Y.-Z. Cai, P. He, J.-C. Shu, W.-Q. Cao, J. Yuan, 2D MXenes: electromagnetic property for microwave absorption and electromagnetic interference shielding, Chem. Eng. J. 359 (2019) 1265–1302.

[28] Y. Li, F. Meng, Y. Mei, H. Wang, Y. Guo, Y. Wang, F. Peng, F. Huang, Z. Zhou, Electrospun generation of $Ti_3C_2T_x$ MXene@graphene oxide hybrid aerogel microspheres for tunable high-performance microwave absorption, Chem. Eng. J. 391 (2020), 123512.

[29] P. Sambyal, A. Iqbal, J. Hong, H. Kim, M.-K. Kim, S.M. Hong, M. Han, Y. Gogotsi, C.M. Koo, Ultralight and mechanically robust $Ti_3C_2T_x$ hybrid aerogel reinforced by carbon nanotubes for electromagnetic interference shielding, ACS Appl. Mater. Interfaces 11 (2019) 38046–38054.

[30] X. Li, C. Wen, L. Yang, R. Zhang, X. Li, Y. Li, R. Che, MXene/FeCo films with distinct and tunable electromagnetic wave absorption by morphology control and magnetic anisotropy, Carbon 175 (2021) 509–518.

[31] M. Peng, F. Qin, Clarification of basic concepts for electromagnetic interference shielding effectiveness, J. Appl. Phys. 130 (2021), 225108.

[32] U. Hwang, J. Kim, M. Seol, B. Lee, I.-K. Park, J. Suhr, J.-D. Nam, Quantitative interpretation of electromagnetic interference shielding efficiency: is it really a wave absorber or a reflector? ACS Omega 7 (2022) 4135–4139.

[33] Z. Zhang, Z. Cai, Y. Zhang, Y. Peng, Z. Wang, L. Xia, S. Ma, Z. Yin, R. Wang, Y. Cao, Z. Li, Y. Huang, The recent progress of MXene-based microwave absorption materials, Carbon 174 (2021) 484–499.

[34] P. He, X.-X. Wang, Y.-Z. Cai, J.-C. Shu, Q.-L. Zhao, J. Yuan, M.-S. Cao, Tailoring $Ti_3C_2T_x$ nanosheets to tune local conductive network as an environmentally friendly material for highly efficient electromagnetic interference shielding, Nanoscale 11 (2019) 6080–6088.

[35] X.-Y. Fang, X.-X. Yu, H.-M. Zheng, H.-B. Jin, L. Wang, M.-S. Cao, Temperature- and thickness-dependent electrical conductivity of few-layer graphene and graphene nanosheets, Phys. Lett. A 379 (2015) 2245–2251.

[36] M. Han, C.E. Shuck, A. Singh, Y. Yang, A.C. Foucher, A. Goad, B. McBride, S. J. May, V.B. Shenoy, E.A. Stach, Y. Gogotsi, Efficient microwave absorption with $V_{n+1}C_nT_x$ MXenes, Cell Rep. Phys. Sci. 3 (2022), 101073.

[37] M. Khazaei, M. Arai, T. Sasaki, C.Y. Chung, N.S. Venkataramanan, M. Estili, Y. Sakka, Y. Kawazoe, Novel electronic and magnetic properties of two-dimensional transition metal carbides and nitrides, Adv. Funct. Mater. 23 (2013) 2185–2192.

[38] H. Weng, A. Ranjbar, Y. Liang, Z. Song, M. Khazaei, S. Yunoki, M. Arai, Y. Kawazoe, Z. Fang, X. Dai, Large-gap two-dimensional topological insulator in oxygen functionalized MXene, Phys. Rev. B 92 (2015), 075436.

[39] A. Lipatov, A. Goad, M.J. Loes, N.S. Vorobeva, J. Abourahma, Y. Gogotsi, A. Sinitskii, High electrical conductivity and breakdown current density of individual monolayer $Ti_3C_2T_x$ MXene flakes, Matter 4 (2021) 1413–1427.

[40] A. Lipatov, M. Alhabeb, M.R. Lukatskaya, A. Boson, Y. Gogotsi, A. Sinitskii, Effect of synthesis on quality, electronic properties and environmental stability of individual monolayer Ti_3C_2 MXene flakes, Adv. Electron. Mater. 2 (2016), 1600255.

[41] T.S. Mathis, K. Maleski, A. Goad, A. Sarycheva, M. Anayee, A.C. Foucher, K. Hantanasirisakul, C.E. Shuck, E.A. Stach, Y. Gogotsi, Modified MAX phase synthesis for environmentally stable and highly conductive Ti_3C_2 MXene, ACS Nano 15 (2021) 6420–6429.

[42] M. Shekhirev, J. Busa, C.E. Shuck, A. Torres, S. Bagheri, A. Sinitskii, Y. Gogotsi, Ultralarge flakes of $Ti_3C_2T_x$ MXene via soft delamination, ACS Nano 16 (2022) 13695–13703.

[43] A. Lipatov, M. Alhabeb, H. Lu, S. Zhao, M.J. Loes, N.S. Vorobeva, Y. Dall'Agnese, Y. Gao, A. Gruverman, Y. Gogotsi, A. Sinitskii, Electrical and elastic properties of individual single-layer $Nb_4C_3T_x$ MXene flakes, Adv. Electron. Mater. 6 (2020), 1901382.

[44] S. Zhao, C. Chen, X. Zhao, X. Chu, F. Du, G. Chen, Y. Gogotsi, Y. Gao, Y. Dall'Agnese, Flexible $Nb_4C_3T_x$ film with large interlayer spacing for high-performance supercapacitors, Adv. Funct. Mater. 30 (2020), 2000815.

[45] C.E. Shuck, M. Han, K. Maleski, K. Hantanasirisakul, S.J. Kim, J. Choi, W.E. Reil, Y. Gogotsi, Effect of Ti_3AlC_2 MAX phase on structure and properties of resultant $Ti_3C_2T_x$ MXene, ACS Appl. Nano Mater. 2 (2019) 3368–3376.

[46] A.D. Dillon, M.J. Ghidiu, A.L. Krick, J. Griggs, S.J. May, Y. Gogotsi, M. W. Barsoum, A.T. Fafarman, Highly conductive optical quality solution-processed films of 2D titanium carbide, Adv. Funct. Mater. 26 (2016) 4162–4168.

[47] M. Han, Y. Liu, R. Rakhmanov, C. Israel, M.A.S. Tajin, G. Friedman, V. Volman, A. Hoorfar, K.R. Dandekar, Y. Gogotsi, Solution-processed $Ti_3C_2T_x$ MXene antennas for radio-frequency communication, Adv. Mater. 33 (2021), 2003225.

[48] J. Lipton, J.A. Röhr, V. Dang, A. Goad, K. Maleski, F. Lavini, M. Han, E.H.R. Tsai, G.-M. Weng, J. Kong, E. Riedo, Y. Gogotsi, A.D. Taylor, Scalable, highly conductive, and micropatternable MXene films for enhanced electromagnetic interference shielding, Matter 3 (2020) 546–557.

[49] C.J. Zhang, L. McKeon, M.P. Kremer, S.-H. Park, O. Ronan, A. Seral-Ascaso, S. Barwich, C.Ó. Coileáin, N. McEvoy, H.C. Nerl, Additive-free MXene inks and direct printing of micro-supercapacitors, Nat. Commun. 10 (2019) 1795.

[50] S. Abdolhosseinzadeh, R. Schneider, A. Verma, J. Heier, F. Nüesch, C. Zhang, Turning trash into treasure: additive free MXene sediment inks for screen-printed micro-supercapacitors, Adv. Mater. 32 (2020), 2000716.

[51] D. Zhou, M. Han, B. Sidnawi, Q. Wu, Y. Gogotsi, B. Li, Ultrafast assembly and healing of nanomaterial networks on polymer substrates for flexible hybrid electronics, Appl. Mater. Today 22 (2021), 100956.

[52] S.J. Kim, J. Choi, K. Maleski, K. Hantanasirisakul, H.-T. Jung, Y. Gogotsi, C. W. Ahn, Interfacial assembly of ultrathin, functional MXene films, ACS Appl. Mater. Interfaces 11 (2019) 32320–32327.

[53] W. Yang, J. Yang, J.J. Byun, F.P. Moissinac, J. Xu, S.J. Haigh, M. Domingos, M. A. Bissett, R.A. Dryfe, S. Barg, 3D printing of freestanding MXene architectures for current-collector-free supercapacitors, Adv. Mater. 31 (2019), 1902725.

[54] Y.-Z. Zhang, Y. Wang, Q. Jiang, J.K. El-Demellawi, H. Kim, H.N. Alshareef, MXene printing and patterned coating for device applications, Adv. Mater. 32 (2020), 1908486.

[55] J. Wang, Y. Liu, Y. Yang, J. Wang, H. Kang, H. Yang, D. Zhang, Z. Cheng, Z. Xie, H. Tan, Z. Fan, A weldable MXene film assisted by water, Matter 5 (2022) 1042–1055.

[56] K. Matthews, T. Zhang, C.E. Shuck, A. VahidMohammadi, Y. Gogotsi, Guidelines for synthesis and processing of chemically stable two-dimensional V_2CT_x MXene, Chem. Mater. 34 (2022) 499–509.

[57] J.L. Hart, K. Hantanasirisakul, A.C. Lang, B. Anasori, D. Pinto, Y. Pivak, J.T. van Omme, S.J. May, Y. Gogotsi, M.L. Taheri, Control of MXenes' electronic properties through termination and intercalation, Nat. Commun. 10 (2019) 522.

[58] Y. Yang, K. Hantanasirisakul, N.C. Frey, B. Anasori, R.J. Green, P.C. Rogge, I. Waluyo, A. Hunt, P. Shafer, E. Arenholz, V.B. Shenoy, Y. Gogotsi, S.J. May, Distinguishing electronic contributions of surface and sub-surface transition metal atoms in Ti-based MXenes, 2D Mater. 7 (2020), 025015.

[59] Y. Yang, M. Han, C.E. Shuck, R.K. Sah, J.R. Paudel, A.X. Gray, Y. Gogotsi, S. J. May, Correlating electronic properties with M-site composition in solid solution $Ti_yNb_{2-y}CT_x$ MXenes, 2D Mater 10 (2023) 014011.

[60] Z. Ling, C.E. Ren, M.-Q. Zhao, J. Yang, J.M. Giammarco, J. Qiu, M.W. Barsoum, Y. Gogotsi, Flexible and conductive MXene films and nanocomposites with high capacitance, Proc. Natl. Acad. Sci. USA 111 (2014) 16676–16681.

[61] S. Wan, X. Li, Y. Wang, Y. Chen, X. Xie, R. Yang, A.P. Tomsia, L. Jiang, Q. Cheng, Strong sequentially bridged MXene sheets, Proc. Natl. Acad. Sci. USA 117 (2020) 27154–27161.

[62] S. Wan, X. Li, Y. Chen, N. Liu, Y. Du, S. Dou, L. Jiang, Q. Cheng, High-strength scalable MXene films through bridging-induced densification, Science 374 (2021) 96–99.

[63] S. Lee, E.H. Kim, S. Yu, H. Kim, C. Park, S.W. Lee, H. Han, W. Jin, K. Lee, C.E. Lee, J. Jang, C.M. Koo, C. Park, Polymer-laminated $Ti_3C_2T_x$ MXene electrodes for transparent and flexible field-driven electronics, ACS Nano 15 (2021) 8940–8952.

[64] Z. Zhou, Q. Song, B. Huang, S. Feng, C. Lu, Facile fabrication of densely packed Ti_3C_2 MXene/nanocellulose composite films for enhancing electromagnetic interference shielding and electro-/photothermal performance, ACS Nano 15 (2021) 12405–12417.

[65] G.-M. Weng, J. Li, M. Alhabeb, C. Karpovich, H. Wang, J. Lipton, K. Maleski, J. Kong, E. Shaulsky, M. Elimelech, Y. Gogotsi, A.D. Taylor, Layer-by-layer assembly of cross-functional semi-transparent MXene-carbon nanotubes composite films for next-generation electromagnetic interference shielding, Adv. Funct. Mater. 28 (2018), 1803360.

[66] J. Zhang, N. Kong, S. Uzun, A. Levitt, S. Seyedin, P.A. Lynch, S. Qin, M. Han, W. Yang, J. Liu, X. Wang, Y. Gogotsi, J.M. Razal, Scalable manufacturing of free-standing, strong $Ti_3C_2T_x$ MXene films with outstanding conductivity, Adv. Mater. 32 (2020), 2001093.

[67] J. Halim, I. Persson, E.J. Moon, P. Kühne, V. Darakchieva, P.O.Å. Persson, P. Eklund, J. Rosen, M.W. Barsoum, Electronic and optical characterization of 2D Ti_2C and Nb_2C (MXene) thin films, J. Phys. Condens. Matter 31 (2019), 165301.

[68] S. Tu, Q. Jiang, X. Zhang, H.N. Alshareef, Large dielectric constant enhancement in MXene percolative polymer composites, ACS Nano 12 (2018) 3369–3377.

[69] S. Tu, Q. Jiang, J. Zhang, X. He, M.N. Hedhili, X. Zhang, H.N. Alshareef, Enhancement of dielectric permittivity of $Ti_3C_2T_x$ MXene/polymer composites by controlling flake size and surface termination, ACS Appl. Mater. Interfaces 11 (2019) 27358–27362.

[70] S.A. Mirkhani, A. Shayesteh Zeraati, E. Aliabadian, M. Naguib, U. Sundararaj, High dielectric constant and low dielectric loss via poly(vinyl alcohol)/$Ti_3C_2T_x$ MXene nanocomposites, ACS Appl. Mater. Interfaces 11 (2019) 18599–18608.

[71] P. He, M.-S. Cao, J.-C. Shu, Y.-Z. Cai, X.-X. Wang, Q.-L. Zhao, J. Yuan, Atomic layer tailoring titanium carbide MXene to tune transport and polarization for utilization of electromagnetic energy beyond solar and chemical energy, ACS Appl. Mater. Interfaces 11 (2019) 12535–12543.

[72] T. Yun, H. Kim, A. Iqbal, Y.S. Cho, G.S. Lee, M.K. Kim, S.J. Kim, D. Kim, Y. Gogotsi, S.O. Kim, C.M. Koo, Electromagnetic shielding of monolayer MXene assemblies, Adv. Mater. 32 (2020), e1906769.

[73] M. Han, C.E. Shuck, R. Rakhmanov, D. Parchment, B. Anasori, C.M. Koo, G. Friedman, Y. Gogotsi, Beyond $Ti_3C_2T_x$: MXenes for electromagnetic interference shielding, ACS Nano 14 (2020) 5008–5016.

[74] A. Iqbal, F. Shahzad, K. Hantanasirisakul, M.-K. Kim, J. Kwon, J. Hong, H. Kim, D. Kim, Y. Gogotsi, C.M. Koo, Anomalous absorption of electromagnetic waves by 2D transition metal carbonitride Ti_3CNT_x (MXene), Science 369 (2020) 446–450.

[75] A. Lipatov, H. Lu, M. Alhabeb, B. Anasori, A. Gruverman, Y. Gogotsi, A. Sinitskii, Elastic properties of 2D $Ti_3C_2T_x$ MXene monolayers and bilayers, Sci. Adv. 4 (2018), eaat0491.

[76] Z. Ma, S. Kang, J. Ma, L. Shao, Y. Zhang, C. Liu, A. Wei, X. Xiang, L. Wei, J. Gu, Ultraflexible and mechanically strong double-layered aramid nanofiber–$Ti_3C_2T_x$ MXene/silver nanowire nanocomposite papers for high-performance electromagnetic interference shielding, ACS Nano 14 (2020) 8368–8382.

[77] W. Chen, L.-X. Liu, H.-B. Zhang, Z.-Z. Yu, Flexible, transparent, and conductive $Ti_3C_2T_x$ MXene–silver nanowire films with smart acoustic sensitivity for high-performance electromagnetic interference shielding, ACS Nano 14 (2020) 16643–16653.

[78] S. Bai, X. Guo, X. Zhang, X. Zhao, H. Yang, $Ti_3C_2T_x$ MXene-AgNW composite flexible transparent conductive films for EMI shielding, Compos. Part A-Appl. S. 149 (2021), 106545.

[79] R. Yang, X. Gui, L. Yao, Q. Hu, L. Yang, H. Zhang, Y. Yao, H. Mei, Z. Tang, Ultrathin, lightweight, and flexible CNT buckypaper enhanced using MXenes for electromagnetic interference shielding, Nano-Micro Lett. 13 (2021) 66.

[80] Z. Xiang, Y. Shi, X. Zhu, L. Cai, W. Lu, Flexible and waterproof 2D/1D/0D construction of MXene-based nanocomposites for electromagnetic wave absorption, EMI shielding, and photothermal conversion, Nano-Micro Lett. 13 (2021) 150.

[81] W.-T. Cao, F.-F. Chen, Y.-J. Zhu, Y.-G. Zhang, Y.-Y. Jiang, M.-G. Ma, F. Chen, Binary strengthening and toughening of MXene/cellulose nanofiber composite paper with nacre-inspired structure and superior electromagnetic interference shielding properties, ACS Nano 12 (2018) 4583–4593.

[82] Z. Cui, C. Gao, Z. Fan, J. Wang, Z. Cheng, Z. Xie, Y. Liu, Y. Wang, Lightweight MXene/cellulose nanofiber composite film for electromagnetic interference shielding, J. Electron. Mater. 50 (2021) 2101–2110.

[83] N. Wu, Z. Zeng, N. Kummer, D. Han, R. Zenobi, G. Nyström, Ultrafine cellulose nanofiber-assisted physical and chemical cross-linking of MXene sheets for electromagnetic interference shielding, Small Methods 5 (2021), 2100889.

[84] P. He, M.-S. Cao, Y.-Z. Cai, J.-C. Shu, W.-Q. Cao, J. Yuan, Self-assembling flexible 2D carbide MXene film with tunable integrated electron migration and group relaxation toward energy storage and green EMI shielding, Carbon 157 (2020) 80–89.

[85] S. Uzun, M. Han, C.J. Strobel, K. Hantanasirisakul, A. Goad, G. Dion, Y. Gogotsi, Highly conductive and scalable $Ti_3C_2T_x$-coated fabrics for efficient electromagnetic interference shielding, Carbon 174 (2021) 382–389.

[86] M. Han, X. Yin, K. Hantanasirisakul, X. Li, A. Iqbal, C.B. Hatter, B. Anasori, C. M. Koo, T. Torita, Y. Soda, L. Zhang, L. Cheng, Y. Gogotsi, Anisotropic MXene aerogels with a mechanically tunable ratio of electromagnetic wave reflection to absorption, Adv. Opt. Mater. 7 (2019), 1900267.

[87] X. Jia, B. Shen, L. Zhang, W. Zheng, Construction of compressible polymer/ MXene composite foams for high-performance absorption-dominated electromagnetic shielding with ultra-low reflectivity, Carbon 173 (2021) 932–940.

[88] S. Zhao, H.-B. Zhang, J.-Q. Luo, Q.-W. Wang, B. Xu, S. Hong, Z.-Z. Yu, Highly electrically conductive three-dimensional $Ti_3C_2T_x$ MXene/reduced graphene oxide hybrid aerogels with excellent electromagnetic interference shielding performances, ACS Nano 12 (2018) 11193–11202.

[89] Z. Lin, J. Liu, W. Peng, Y. Zhu, Y. Zhao, K. Jiang, M. Peng, Y. Tan, Highly stable 3D $Ti_3C_2T_x$ MXene-based foam architectures toward high-performance terahertz radiation shielding, ACS Nano 14 (2020) 2109–2117.

[90] P. Miles, W. Westphal, A. Von Hippel, Dielectric spectroscopy of ferromagnetic semiconductors, Rev. Mod. Phys. 29 (1957) 279.

[91] Y. Cui, Z. Liu, Y. Zhang, P. Liu, M. Ahmad, Q. Zhang, B. Zhang, Wrinkled three-dimensional porous MXene/Ni composite microspheres for efficient broadband microwave absorption, Carbon 181 (2021) 58–68.

[92] F. Pan, L. Yu, Z. Xiang, Z. Liu, B. Deng, E. Cui, Z. Shi, X. Li, W. Lu, Improved synergistic effect for achieving ultrathin microwave absorber of 1D Co nanochains/2D carbide MXene nanocomposite, Carbon 172 (2021) 506–515.

[93] B. Deng, Z. Liu, F. Pan, Z. Xiang, X. Zhang, W. Lu, Electrostatically self-assembled two-dimensional magnetized MXene/hollow Fe_3O_4 nanoparticle hybrids with high electromagnetic absorption performance and improved impendence matching, J. Mater. Chem. A 9 (2021) 3500–3510.

[94] C. Wen, X. Li, R. Zhang, C. Xu, W. You, Z. Liu, B. Zhao, R. Che, High-density anisotropy magnetism enhanced microwave absorption performance in $Ti_3C_2T_x$ MXene@Ni microspheres, ACS Nano 16 (2021) 1150–1159.

[95] M. Li, M. Han, J. Zhou, Q. Deng, X. Zhou, J. Xue, S. Du, X. Yin, Q. Huang, Novel scale-like structures of graphite/TiC/Ti_3C_2 hybrids for electromagnetic absorption, Adv. Electron. Mater. 4 (2018), 1700617.

[96] L. Kong, J. Qi, M. Li, X. Chen, X. Yuan, T. Wang, J. Yang, J. Huang, X. Fan, Electromagnetic wave absorption properties of $Ti_3C_2T_x$ nanosheets modified with in-situ growth carbon nanotubes, Carbon 183 (2021) 322–331.

[97] Z. Wu, Z. Yang, C. Jin, Y. Zhao, R. Che, Accurately engineering 2D/2D/0D heterojunction in hierarchical $Ti_3C_2T_x$ MXene nanoarchitectures for electromagnetic wave absorption and shielding, ACS Appl. Mater. Interfaces 13 (2021) 5866–5876.

[98] W. Zhu, F. Ye, M. Li, X. Wang, Q. Zhou, X. Fan, J. Xue, X. Li, In-situ growth of wafer-like Ti_3C_2/Carbon nanoparticle hybrids with excellent tunable electromagnetic absorption performance, Compos. B Eng. 202 (2020), 108408.

[99] L. Wang, H. Liu, X. Lv, G. Cui, G. Gu, Facile synthesis 3D porous MXene $Ti_3C_2T_x$@ RGO composite aerogel with excellent dielectric loss and electromagnetic wave absorption, J. Alloys Compd. 828 (2020), 154251.

[100] J. Wang, L. Liu, S. Jiao, K. Ma, J. Lv, J. Yang, Hierarchical carbon Fiber@MXene@ MoS_2 core-sheath synergistic microstructure for tunable and efficient microwave absorption, Adv. Funct. Mater. 30 (2020), 2002595.

[101] T. Hou, Z. Jia, B. Wang, H. Li, X. Liu, L. Bi, G. Wu, MXene-based accordion 2D hybrid structure with Co_9S_8/C/$Ti_3C_2T_x$ as efficient electromagnetic wave absorber, Chem. Eng. J. 414 (2021), 128875.

[102] L. Ma, M. Hamidinejad, C. Liang, B. Zhao, S. Habibpour, A. Yu, T. Filleter, C. B. Park, Enhanced electromagnetic wave absorption performance of polymer/SiC-nanowire/MXene ($Ti_3C_2T_x$) composites, Carbon 179 (2021) 408–416.

[103] M. Li, W. Zhu, X. Li, H. Xu, X. Fan, H. Wu, F. Ye, J. Xue, X. Li, L. Cheng, L. Zhang, $Ti_3C_2T_x$/MoS_2 self-rolling rod-based foam boosts interfacial polarization for electromagnetic wave absorption, Adv. Sci. 9 (2022), 2201118.

[104] L. Liang, Q. Li, X. Yan, Y. Feng, Y. Wang, H.-B. Zhang, X. Zhou, C. Liu, C. Shen, X. Xie, Multifunctional magnetic $Ti_3C_2T_x$ MXene/graphene aerogel with superior electromagnetic wave absorption performance, ACS Nano 15 (2021) 6622–6632.

[105] X. Li, X. Yin, C. Song, M. Han, H. Xu, W. Duan, L. Cheng, L. Zhang, Self-assembly core-shell graphene-bridged hollow MXenes spheres 3D foam with ultrahigh specific EM absorption performance, Adv. Funct. Mater. 28 (2018), 1803938.

[106] X.-X. Wang, M. Zhang, J.-C. Shu, B. Wen, W.-Q. Cao, M.-S. Cao, Thermally-tailoring dielectric "genes" in graphene-based heterostructure to manipulate electromagnetic response, Carbon 184 (2021) 136–145.

[107] M. Cao, X. Wang, W. Cao, X. Fang, B. Wen, J. Yuan, Thermally driven transport and relaxation switching self-powered electromagnetic energy conversion, Small 14 (2018), 1800987.

[108] M.-S. Cao, J.-C. Shu, B. Wen, X.-X. Wang, W.-Q. Cao, Genetic dielectric genes inside 2D carbon-based materials with tunable electromagnetic function at elevated temperature, Small Structures 2 (2021), 2100104.

[109] C. Cui, R. Guo, E. Ren, H. Xiao, M. Zhou, X. Lai, Q. Qin, S. Jiang, W. Qin, MXene-based rGO/Nb_2CT_x/Fe_3O_4 composite for high absorption of electromagnetic wave, Chem. Eng. J. 405 (2021), 126626.